Bioorganic & Medicinal Chemistry Letters 22 (2012) 1014–1018

Contents lists available at SciVerse ScienceDirect

Bioorganic & Medicinal Chemistry Letters

journal homepage: www.elsevier.com/locate/bmcl

The discovery of potent antagonists of NPBWR1 (GPR7)

F. Anthony Romero [a,*], Nicholas B. Hastings [b], Remond Moningka [a], Zhiqiang Guo [a], Ming Wang [a], Jerry Di Salvo [c], Ying Lei [c], Dorina Trusca [c], Qiaolin Deng [d], Vincent Tong [e], Jenna L. Terebetski [f], Richard G. Ball [g], Feroze Ujjainwalla [a]

[a] Merck & Co., Inc., Department of Medicinal Chemistry, PO Box 2000, Rahway, NJ 07065, USA
[b] Merck & Co., Inc., Department of Neuroscience and Ophthalmology, Kenilworth, NJ 07033, USA
[c] Merck & Co., Inc., Department of In Vitro Pharmacology, PO Box 2000, Rahway, NJ 07065, USA
[d] Merck & Co., Inc., Department of Chemistry Modeling and Informatics , PO Box 2000, Rahway, NJ 07065, USA
[e] Merck & Co., Inc., Department of Pharmacokinetics, Pharmacodynamics, and Drug Metabolism, PO Box 2000, Rahway, NJ 07065, USA
[f] Merck & Co., Inc., Department of Basic Pharmaceutical Sciences, PO Box 2000, Rahway, NJ 07065, USA
[g] Merck & Co., Inc., Department of Analytical Chemistry, PO Box 2000, Rahway, NJ 07065, USA

ARTICLE INFO

Article history:
Received 27 October 2011
Revised 29 November 2011
Accepted 30 November 2011
Available online 8 December 2011

Keywords:
NPBWR1
GPR7
Antagonist
Anti-obesity
G protein-coupled receptor

ABSTRACT

The synthesis and evaluation of small molecule antagonists of the G protein-coupled receptor NPBWR1 (GPR7) are reported for the first time. [4-(5-Chloropyridin-2-yl)piperazin-1-yl][(1*S*,2*S*,4*R*)-4-{[(1*R*)-1-(4-methoxyphenyl)ethyl]amino}-2-(thiophen-3-yl)cyclohexyl]methanone (**1**) emerged as a hit from a high-throughput screen. Examination of substituents that focused on replacing the 5-chloropyridine and 4-methoxybenzylamino groups of **1** led to the identification of compounds that exhibited subnanomolar potencies as low as 660 pM (**9k**) in the functional assay and 200 pM in the binding assay (**9i**).

In 2002, G protein-coupled receptor 7 (GPR7) was deorphanized with the identification of endogenous ligands neuropeptide B (NPB) and neuropeptide W (NPW).[1] Shortly thereafter it was reclassified as Neuropeptide B/W receptor-1 (NPBWR1). Since the deorphanization there have been several studies that have suggested NPBWR1 to be involved in feeding behavior, energy homeostasis, neuroendocrine function, and modulating inflammatory pain.[2]

In humans and rodents, mRNA encoding NPBWR1 and it's ligands NPB and NPW have been found to be co-localized in peripheral tissues (alimentary tract and endocrine system), but are mainly concentrated within the central nervous system (CNS). NPBWR1 appears to be abundant in the hippocampus, subcortical limbic telencephalon, hypothalamus, olfactory cortex, midbrain periaqueductal gray and tegmental area.[3] These regions correspond well to the localization of NPB-/NPW-immunoreactive processes to ligand binding sites localized using radioiodinated NPB in rat brain or NPW in mouse brain, as well as regions in which cFos immunoreactivity is enhanced following intracerebroventricular (i.c.v.) administration of NPW to the rat.[3–8] These observations suggest that the NPBWR1 receptor may be involved in cognitive and affective reactions to stress, arousal, locomotor activity, cardiovascular and neuroendocrine responses, as well as energy homeostasis.

Among the pharmacological effects of NPB and NPW we were primarily interested in their effects on food intake and body weight. Studies have shown that i.c.v. injection of NPW in rats caused acute hyperphagia in male rats while i.c.v. injection of NPB increased feeding.[1c,d] As such, NPBWR1 has emerged as an interesting new therapeutic target. In an effort to probe NPBWR1 as a novel anti-obesity target we wished to develop a small 'molecule antagonist.

To date no known small molecule antagonists of NPBWR1 have been reported in the literature. In an effort to validate NPBWR1 as

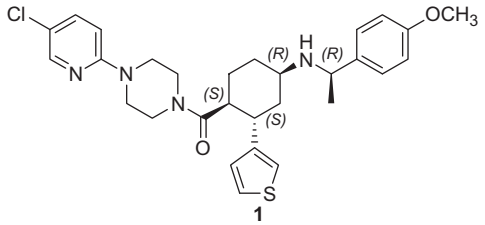

1

mouse cAMP / binding IC_{50} = 363 / 25 nM
human cAMP / binding IC_{50} = 1925 / 324 nM

Figure 1. In vitro potency of lead compound **1** at mouse and human NPBWR1.

* Corresponding author. Tel.: +1 732 594 6040.
E-mail address: anthony_romero@merck.com (F. Anthony Romero).

0960-894X/$ - see front matter © 2011 Elsevier Ltd. All rights reserved.
doi:10.1016/j.bmcl.2011.11.126

an anti-obesity target, we started a discovery program aimed at developing a small molecule antagonist as a pharmacological tool. In this regard, a high-throughput screen was performed of the Merck collection. One lead that emerged from this screen was compound **1** (Fig. 1). This compound exhibited moderate potency (IC_{50} = 363 nM) in a mouse functional cyclic-AMP (cAMP) assay and was shown in our mouse binding assay to be relatively potent with an IC_{50} of 25 nM. While the human in vitro potency was shifted toward weaker potency by 13- and 5-fold in the cAMP and binding assays, respectively, our primary interest was in identifying a tool compound that would be suitable in a mouse in vivo model to probe the mechanism of NPBWR1. Compound **1** was evaluated in both mouse liver microsomes and Pgp efflux studies (LLC-PK1:MDR1 cell line). Compound **1** was found to have poor intrinsic metabolic stability (0% parent remaining at 30 min) and was also found to be a Pgp substrate. The limited metabolic stability of **1** coupled with it also being a Pgp substrate precluded it from further pharmacokinetic studies and being used as an in vivo tool that could be administered peripherally (po or iv). As the initial structure–activity relationships (SAR) of **1** were being developed, many of these compounds were also shown to be have limited metabolic stability and were also Pgp substrates (data not shown) thus decreasing the chance of sufficient iv or po exposure in the CNS. An alternative method for dosing we considered was through an i.c.v. route since we were targeting NPBWR1 in the CNS and metabolic stability Pgp efflux would not be an issue. We had decided early on in this program to develop a compound that could be used as an i.c.v. tool, thus we sought to optimize compound **1** on in vitro potency. For the purposes of this article the potencies described will be at the mouse receptor unless otherwise indicated. Here we report the optimization of **1** at mouse NPBWR1, the identification of the first potent antagonists of NPBWR1 and the identification of candidate pharmacological in vivo tool compounds.

Key to the divergent synthesis[9] of the antagonists was the preparation of intermediate *ent*-**5** from which all the requisite compounds could be synthesized (Scheme 1). A Diels–Alder reaction between 2-trimethylsilyloxy-1,3-butadiene and cinnamyl ester **2** followed by treatment with HCl produced two cyclohexanone regioisomers **3** and **4** in a 3:1 ratio, respectively. Compound **3** was the major product and was easily separable from **4** by silica gel chromatography. Hydrolysis of the pentafluorophenyl ester and resolution on a preparative SFC chiral column yielded enantiopure intermediate *ent*-**5**. Intermediate *ent*-**5** underwent amide coupling with the appropriate aryl substituted piperazine with use of a resin bound coupling agent to produce *ent*-**6**. After filtration of the resin and evaporation of the solvent, the crude coupling product was then subjected to reductive amination with the appropriate amine by enlisting resin bound cyanoborohydride to afford two diastereomers (3:2 ratio; **7–9** : **10**) of which the major diastereomer (**7–9**) was the one we required. The diastereomers **7–9** and **10** were easily separated by reverse phase HPLC to provide the requisite candidate antagonists (**7a–o**, **8a–n** and **9a–k**).[10] The absolute stereochemistry of the final compounds was determined by obtaining an X-ray crystal structure of compound **8f** (Fig. 2; CCDC 854950).[11]

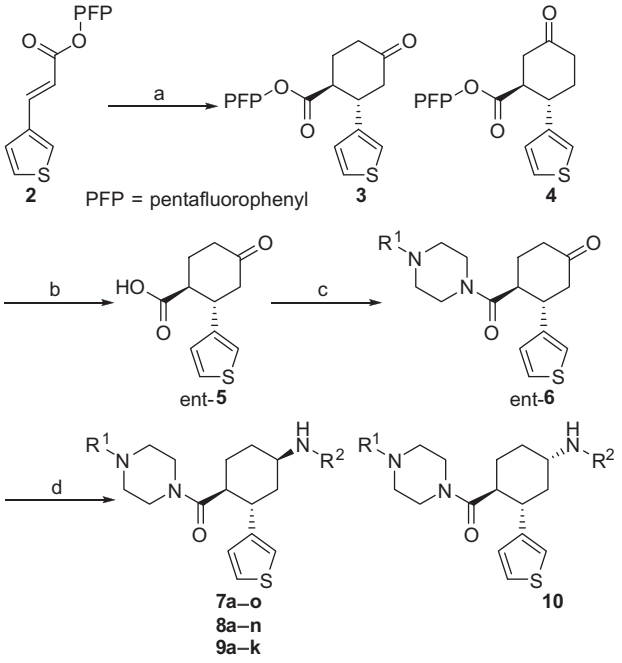

Scheme 1. Reagents and conditions: (a) 2-trimethylsilyloxy-1,3-butadiene, 150 °C sealed tube, 24 h then 3 N HCl; (b) LiOH then SFC AD-H column; (c) R^1-piperazine, PS-carbodiimide, HOBT; (d) R^2-NH_2, MP-cyanoborohydride, AcOH.

The structure–activity relationships (SAR) of compound **1** focused on left-hand aryl ring (Fig. 3) and right-hand benzylamine (Fig. 4). To explore the left-hand aryl moiety a systematic series of modifications were made and some key interactions emerged from this series (Fig. 3, **7a**–**o**). Removal of the pyridine nitrogen of **1**, compound **7a**, proved detrimental to activity and resulted in a ~10-fold loss in potency. This loss of binding potency proves consistent with a loss in binding affinity due to a hydrogen-bond interaction within the binding site. While removal of the chlorine atom of **1**, compound **7b**, had little effect on the functional potency, the binding affinity decreased by 12-fold. Substitution of the chlorine atom of **1** at different positions around the pyridine ring (**7c**–**e**) resulted in loss of potency. Replacement of the chlorine atom with other lipophilic groups such as a methyl (**7f**) or trifluoromethyl (**7g**) maintained potency as compared to **1** whereas hydrophilic moieties appear to reduce potency significantly. To further explore the putative hydrogen-bonding of the pyridine nitrogen of **1**, we explored a few heterocycles that would position nitrogen similar to the pyridine nitrogen of **1**. Compound **7j** was indistinguishable in potency from **7b** and indicated that replacement of the pyridine with other heterocycles would be tolerated. Placement of a lipophilic substituent on the heterocycle (**7k** and **7l**) increased potency. Attaching a fused phenyl ring to a heterocycle as in **7m–o** led to the largest increase in potency with **7n** notably having a nine-fold increase in binding potency and 20-fold increase in functional activity over lead compound **1**.

Concurrent with these studies, the SAR of the right-hand α-methyl benzylamine was explored (Fig. 4, **8a**–**n**). Removal of the α-methyl substituent resulted in a significant loss in potency. The stereogenic α-methyl was replaced with a *gem*-dimethyl substituent (**8c**) and a two-fold increase in binding potency was observed over **1**. The *gem*-dimethyl substituent may help contribute towards rigidification of the benzyl side chain whereby it orients the 4-methoxyphenyl substituent towards a specific interaction

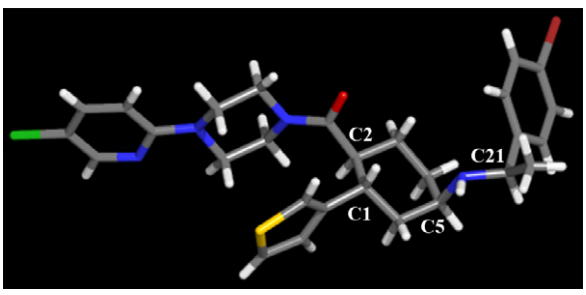

Figure 2. X-ray crystallography analysis confirmed the absolute stereochemistry of compound **8f**. C1, C2, C5, C21 are *S*, *S*, *R*, *R*, respectively.

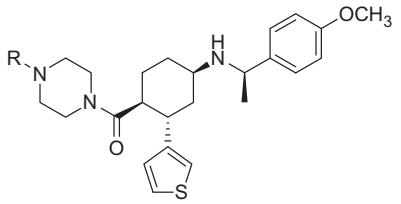

cmpd	R	cAMP IC_{50} (nM)	binding IC_{50} (nM)
1	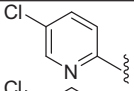	360	25
7a	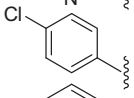	3865	3715
7b	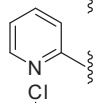	330	290
7c	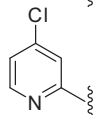	2143	N.D.
7d	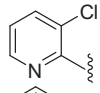	>32000	N.D.
7e	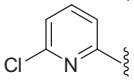	7486	N.D.
7f	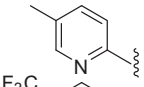	400	74
7g	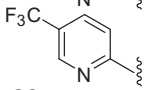	200	18
7h	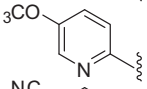	7303	N.D.
7i	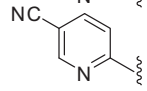	7054	1140
7j	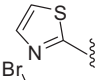	207	194
7k	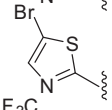	55	14
7l	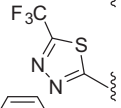	115	42
7m	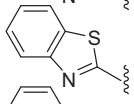	24	4.5
7n	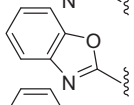	18	2.8
7o	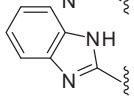	20	8.3

Figure 3. Exploration of the aryl substituent on the piperazine.

in the binding site. This concept was further explored with substitution of a cyclopropyl (**8d**) and cyclobutyl (**8e**) substituent. Unexpectedly, the substitution of a cyclopropyl substitutent (**8d**) led to a five-fold decrease in binding potency compared to **8c**. However, a cyclobutyl substituent (**8e**) proved quite favorable and notably increased binding potency eight-fold over compound

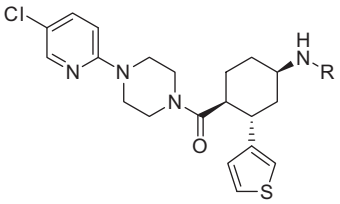

cmpd	R	cAMP IC_{50} (nM)	binding IC_{50} (nM)
1	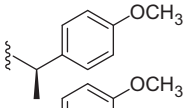	360	25
8a	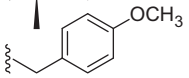	3595	1525
8b	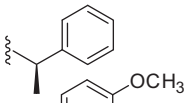	981	217
8c	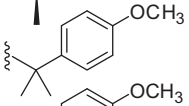	43	11
8d	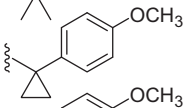	523	56
8e	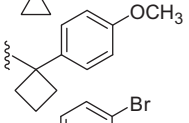	20	3.1
8f	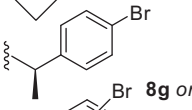	2628	134
8g–i	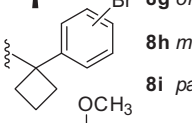	**8g** *ortho* 2208 **8h** *meta* 972 **8i** *para* 601	2196 160 82
8j	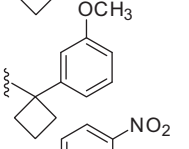	1020	118
8k	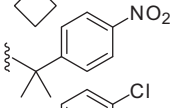	1100	100
8l	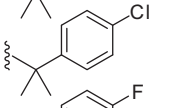	1700	27
8m	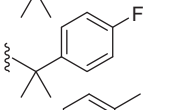	320	17
8n	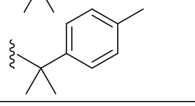	211	16

Figure 4. Exploration of the α-methyl substituent and substitution on the benzyl aryl ring.

1 and 500-fold over compound **8a**. Additional effects of the substituent on the benzyl aryl ring were also examined (**8f–n**). Para substitution was favored on the phenyl ring as indicated by cyclobutyl containing compounds **8e** and **8g–j**. One trend that emerged from examination of substituents in the para position of a series of *gem*-dimethyl containing compounds (**8c** and **8k–n**) was that the binding potency decreased as the substituent on the phenyl ring became more electronegative. Although generalizations are not fully defined by this limited data set, it does appear that electron-donating substituents are more positively impactful on potency than electron-withdrawing substituents. Although the nature of the interaction of the phenyl group in the binding site is unclear, it does not appear to be involved in a π–π interaction because the opposite trend would have been observed.

With the discovery of productive modifications on the left- and right-hand sides of the molecule we sought to combine some of these better substituents (**9a–g**) in the hope of providing a further benefit to potency. Figure 5 summarizes some of these combinations. Gratifyingly, these combinations did indeed provide an enhancement in both functional and binding potency. Compound **9b** exhibited subnanomolar binding affinity and single digit nanomolar functional potency providing a 36-fold and 61-fold increase in binding and functional potency, respectively, compared to the lead compound **1**. Exploration of substitution on the benzoxazole and benzimidazole ring was performed (**9h–k**). While the addition of a methyl substituent matched the potency of unsubstituted benzoxazole **9b**, placement of a fluorine atom on the benzoxazole (**9i** and **9j**) and benzimidazole (**9k**) rings led to the most potent compounds of the series. Both compounds **9i** and **9k** exhibited subnanomolar binding and functional potency. Most notably, compound **9i** resulted in a 420-fold increase in functional potency and 125-fold increase in binding potency over lead compound **1**.

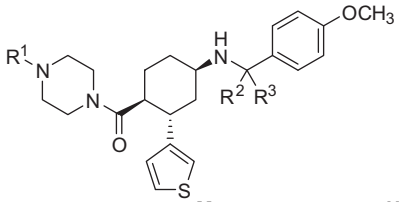

cmpd	R^1	R^2, R^3	Mouse cAMP[a] IC_{50}	Mouse binding[a] IC_{50}	Human cAMP[a] IC_{50}	Human binding[a] IC_{50}
9a	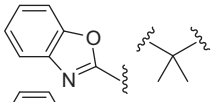		9.2	1.9	110	21
9b	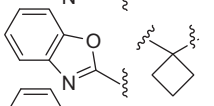		5.9	0.69	40	4.2
9c	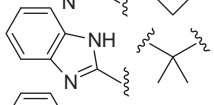		4.6	2.4	39	35
9d	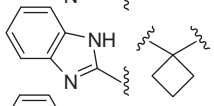		3.0	1.1	11	5.9
9e	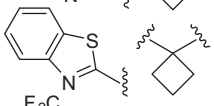		1.8	0.33	N.D.	N.D.
9f	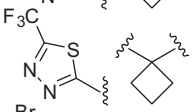		14	2.2	342	95
9g	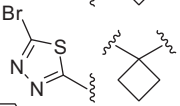		12	2.6	197	18
9h	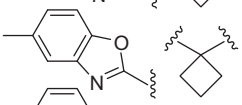		3.9	0.43	70	6.0
9i	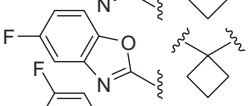		0.86	0.20	N.D.	N.D.
9j	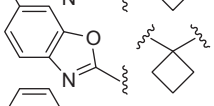		1.3	0.18	N.D.	N.D.
9k	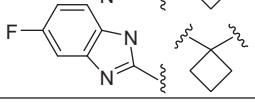		0.66	0.42	N.D.	N.D.

[a] values in nM

Figure 5. Combination of the some of the most potent substituents and substitution on the benzoxazole and benzimidazole rings.

Functional and binding potency at the human receptor were also determined for some of the compounds in Figure 4. As with our initial lead compound (**1**), the human potencies were shifted toward weaker potency between 5- and 43-fold for the binding potencies and between 4- and 24-fold for the functional potencies. Since our goal was to develop a compound to probe target engagement in the mouse, the shift in human potency was not a concern at this stage. Although we had abandoned early on to optimize these compounds for metabolic stability and Pgp efflux we had decided to evaluate compounds **9a–k** as they were some of the most potent compounds. Unfortunately, these compounds were no different as compound **1**. All were Pgp substrates and had <10% parent remaining at 30 min in mouse liver microsomes. In a future publication we will describe our results with the identification of an i.c.v. in vivo tool compound and results on engaging the target.

In summary, we have prepared and evaluated analogues of compound **1** for NPBWR1 antagonist activity. Simultaneous exploration of the aryl group on the piperazine as well as exploration of the benzylamine allowed us to identify groups that were productive towards increasing potency. Combination of these groups and further SAR allowed us to identify the first potent small molecule antagonists of NPBWR1. Most notable of this examination was the substitution of a 5-fluorobenzoxazole for the 5-chloropyridine of **1** and substitution of a spirocyclobutane for the stereogenic methyl of **1** which produced compound **9i** with picomolar potency in both the functional and binding assays. More importantly, several of these antagonists are potential i.c.v. pharmacological in vivo tools that may help elucidate the role of NPBWR1 as an anti-obesity target.

Supplementary data

Supplementary data (methods and conditions for the binding and functional assays) associated with this article can be found, in the online version, at doi:10.1016/j.bmcl.2011.11.126.

References and notes

1. (a) Brezillon, S.; Lannoy, V.; Franssen, J. D.; Le Poul, E.; Dupriez, V.; Lucchetti, J.; Detheux, M.; Parmentier, M. *J. Biol. Chem.* **2003**, *278*, 776; (b) Fujii, R.; Yoshida, H.; Fukusumi, S.; Habata, Y.; Hosoya, M.; Kawamata, Y.; Yano, T.; Hinuma, S.; Kitada, C.; Asami, T.; Mori, M.; Fujisawa, Y.; Fujino, M. *J. Biol. Chem.* **2002**, *277*, 34010; (c) Shimomura, Y.; Harada, M.; Goto, M.; Sugo, T.; Matsumoto, Y.; Abe, M.; Watanabe, T.; Asami, T.; Kitada, C.; Mori, M.; Onda, H.; Fujino, M. *J. Biol. Chem.* **2002**, *277*, 35826; (d) Tanaka, H.; Yoshida, T.; Miyamoto, N.; Motoike, T.; Kuroso, H.; Shibata, K.; Yamanaka, A.; Williams, S. C.; Richardson, S. J.; Tsujino, N.; Garry, M. G.; Lerner, M. R.; King, D. S.; O'Dowd, B. F.; Sakurai, T.; Yanagisawa, M. *Proc. Natl. Acad. Sci. U.S.A.* **2003**, *100*, 6251.
2. Hondo, M.; Ishii, M.; Sakurai, T. *Results Probl. Cell. Differ.* **2008**, *46*, 239.
3. Jackson, V. R.; Lin, S. H.; Wang, Z.; Nothacker, H. P.; Civelli, O. *J. Comp. Neurol.* **2006**, *497*, 367.
4. Kitamura, Y.; Tanaka, H.; Motoike, T.; Ishii, M.; Williams, S. C.; Yanagisawa, M.; Sakurai, T. *Brain Res.* **2006**, *1093*, 123.
5. Schulz, S.; Stumm, R.; Hollt, V. *Neurosci. Lett.* **2007**, *16*, 842.
6. Singh, G.; Maguire, J. J.; Kuc, R. E.; Fidock, M.; Davenport, A. P. *Brain Res.* **2004**, *1017*, 222.
7. Takenoya, F.; Kitamura, S.; Kageyama, H.; Nonaka, N.; Seki, M.; Itabashi, K.; Date, Y.; Nakazato, M.; Shioda, S. *Regul. Pept.* **2008**, *145*, 116.
8. Levine, A.; Winsky-Sommerer, R.; Huitron-Resendiz, S.; Grace, M.; de Lecea, L. *Am. J. Physiol. Regul. Integr. Comp. Physiol.* **2005**, *288*, R1727.
9. Representative experimental procedure (compound **9c**): To a round-bottom flask was added 3-(3-thienyl)acrylic acid (700 mg, 4.54 mmol), pentafluorophenol (1.08 g, 5.90 mmol), EDC (4.04 g, 5.45 mmol), DMAP (55.5 mg, 0.45 mmol) and dichloromethane (23.0 mL) at rt. The resulting mixture was stirred at rt overnight before quenching with 1 N HCl (20 mL). The two phases were separated and the organic layer was washed with saturated aqueous $NaHCO_3$ and brine, and dried over Na_2SO_4, filtered, and concentrated under vacuum. The crude mixture was purified by silica gel chromatography eluting with 0–10% EtOAc/hexanes to give pentafluorophenyl (2*E*)-3-(thiophen-3-yl)prop-2-enoate **2** (1.35 g, 93%) as a white solid. ^{1}H NMR

($CDCl_3$, 500 MHz): δ 7.96 (d, J = 15.9 Hz, 1H), 7.68 (dd, J = 2.7, 1.0 Hz, 1H), 7.44 (dd, J = 5.1, 2.9 Hz, 1H), 7.41 (dd, J = 5.0, 1.2 Hz, 1H), 6.49 (d, J = 15.9 Hz, 1H).

A mixture of pentafluorophenyl (2*E*)-3-(thiophen-3-yl)prop-2-enoate **2** (1.35 g, 4.22 mmol), 2-(trimethylsiloxy)-1,3-butadiene (2.97 mL, 16.7 mmol) and hydroquinone (0.02 g, 0.21 mmol) in toluene (2.81 mL) was heated in a thick-walled glass tube for 24 h at 170 °C. The reaction mixture was allowed to cool to rt and concentrated under vacuum. To the crude mixture in methanol (5 mL) was added 3 N HCl (5 mL) at rt. After 30 min of stirring at rt, the reaction mixture was concentrated under vacuum and then water was added. The resulting mixture was extracted with EtOAc (2×, 50 mL) and the combined extracts were dried over Na_2SO_4, filtered and concentrated under vacuum. The crude residue was purified by silica gel chromatography eluting with 0–95% EtOAc/hexanes to give in order of elution racemic compound **4** (528 mg, 32% yield) as a colorless oil ^{1}H NMR ($CDCl_3$, 500 MHz): δ 7.32 (dd, J = 4.9, 3.0 Hz, 1H), 7.11–7.13 (m, 1H), 7.04 (d, J = 5.0 Hz, 1H), 3.38 (ddd, J = 15.4, 12.3, 3.3 Hz, 1H), 2.89 (ddd, J = 15.5, 12.1, 3.5 Hz, 1H), 2.35 (dt, J = 13.6, 3.3 Hz, 1H), 2.28 (dq, J = 13.7, 6.1, 3.0 Hz, 1H), 2.18 (dq, J = 13.2, 7.1, 3.7 Hz, 1H), 1.93–2.03 (m, 1H), 1.51–1.66 (m, 2H) and racemic compound **3** (731 mg, 44% yield) as a white solid. ^{1}H NMR ($CDCl_3$, 400 MHz): δ 7.32 (dd, J = 5.0, 2.9 Hz, 1H), 7.10–7.13 (m, 1H), 7.01 (dd, J = 4.9, 1.2 Hz, 1H), 3.65 (ddd, J = 15.3, 11.1, 4.8 Hz, 1H), 3.31 (ddd, J = 14.1, 10.3, 3.8 Hz, 1H), 2.75 (ddd, J = 14.8, 4.9, 1.6 Hz, 1H), 2.58–2.68 (m, 2H), 2.50–2.56 (m, 1H), 2.39–2.49 (m, 1H), 2.12–2.25 (m, 1H).

To racemic compound **3** (100 mg, 0.256 mmol) in a mixture of tetrahydrofuran (1921 μL) and water (640 μL) was added LiOH (18.41 mg, 0.769 mmol) in one portion at rt. The reaction mixture was stirred at 60 °C for 2 h. After cooling to rt, the reaction mixture was acidified with 1 N HCl, and poured into water (10 mL). The resulting mixture was extracted with dichloromethane (2×, 50 mL). The combined organic layers were dried over Na_2SO_4, filtered, and concentrated under vacuum. Resolution on a preparative SFC chiral column (AD-3 column, faster eluting isomer) gave enantiopure (1*S*,2*S*)-4-oxo-2-(thiophene-3-yl)cyclohexanecarboxylic acid as a brown solid. ^{1}H NMR ($CDCl_3$, 400 MHz): δ 7.28 (dd, J = 4.9, 2.9 Hz, 1H), 7.04 (d, J = 1.6 Hz, 1H), 6.96 (dd, J = 5.0, 1.1 Hz, 1H), 3.53 (ddd, J = 15.1, 10.8, 4.8 Hz, 1H), 2.96 (ddd, J = 13.7, 10.0, 3.8 Hz, 1H), 2.69 (ddd, J = 14.8, 4.8, 1.6 Hz, 1H), 2.50–2.61 (m, 2H), 2.38–2.48 (m, 1H), 2.20–2.30 (m, 1H), 1.98–2.11 (m, 1H).

(1*S*,2*S*)-4-Oxo-2-(thiophene-3-yl)cyclohexanecarboxylic acid **5** (124 mg, 0.55 mmol) and 2-(piperazin-1-yl)-1*H*-benzimidazole hydrochloride (127 mg, 0.46 mmol) were dissolved in tetrahydrofuran (7.60 mL), and HOBt (106 mg, 0.69 mmol) was added followed by diisopropyl ethyl amine (120 μL, 0.69 mmol) and PS-carbodimide (1.24 g, 1.38 mmol). The reaction mixture was put in a shaker at rt overnight. Upon completion, PS-trisamine (674 mg, 2.30 mmol) was added, and the resulting mixture was further shaken at rt for 2 h. Filtration of the resins followed by evaporation of the solvent afforded crude (3*S*,4*S*)-4-{[4-(1*H*-benzimidazol-2-yl)piperazin-1-yl]carbonyl}-3-(thiophen-3-yl)cyclohexanone, which was used directly in the next step without further purification.

(3*S*,4*S*)-4-{[4-(1*H*-Benzimidazol-2-yl)piperazin-1-yl]carbonyl}-3-(thiophen-3-yl)cyclohexanone (30 mg, 0.07 mmol) was dissolved in a mixture of MeOH (367 μL) and DCE (367 μL), and 2-(4-methoxyphenyl)propan-2-amine (59.2 mg, 0.29 mmol) was added followed by MP-cyanoborohydride (159 mg, 0.367 mmol) and acetic acid (13.0 μL, 0.22 mmol) at rt. The reaction mixture was shaken overnight at 55 °C, cooled to rt, filtered and concentrated under vacuum. LC–MS indicated a 3:2 ratio of diastereomeric reductive amination products. The two diastereomers were separated by reverse phase HPLC (Sunfire prep C18 30 mm × 100 mm) eluting with acetonitrile/water + 0.1% TFA to give [4-(1*H*-benzimidazol-2-yl)piperazin-1-yl][(1*S*,2*S*,4*R*)-4-{[2-(4-methoxyphenyl)propan-2-yl]amino}-2-(thiophen-3-yl)cyclohexyl]methanone TFA salt (**9c**) as a white solid (only the slower eluting isomer was isolated as the desired compound). ^{1}H NMR (CD_3OD, 400 MHz): δ 7.49–7.55 (m, 2H), 7.26 (dd, J = 5.0, 3.0 Hz, 1H), 7.16–7.22 (m, 1H), 7.19 (dd, J = 5.9, 3.2 Hz, 1H), 7.00–7.03 (m, 1H), 6.91–6.99 (m, 5H), 3.80–3.88 (m, 1H), 3.74 (s, 3H), 3.35–3.53 (m, 5H), 3.17–3.33 (m, 2H), 2.92–3.02 (m, 2H), 2.52–2.63 (m, 1H), 1.83–196 (m, 2H), 1.78 (s, 3H), 1.77 (s, 3H), 1.54–1.72 (m, 4H).

10. All eight stereoisomers of compound **1** were evaluated that were derived from the enantiomers of intermediate **5**. Only compound **1** as shown in Figure 1 possessing the *S*, *S*, *R*, *R* configuration was shown to have significant activity. For the purposes of this paper the SAR surrounding this single enantiomer is discussed.
11. In order to determine the absolute configuration of the candidate antagonists we obtained an X-ray structure of compound **8f**. Commercially available (*R*)-4-bromo-α-methylbenzylamine was used in order to establish the absolute configuration of the stereogenic centers in this molecule.